

2024

Application of Haines and Terbrugge chart for suitable slope angles – A case study of Artisanal and small-scale mining

Author(s) ORCID Identifier:

Carol Mgiba:  0009-0004-4464-0461

Steven Rupprecht:  0000-0003-2462-2819

Follow this and additional works at: <https://jsm.gig.eu/journal-of-sustainable-mining>



Part of the [Explosives Engineering Commons](#), [Oil, Gas, and Energy Commons](#), and the [Sustainability Commons](#)

Recommended Citation

Mgiba, Carol and Rupprecht, Steven (2024) "Application of Haines and Terbrugge chart for suitable slope angles – A case study of Artisanal and small-scale mining," *Journal of Sustainable Mining*: Vol. 23 : Iss. 4 , Article 8.

Available at: <https://doi.org/10.46873/2300-3960.1433>

This Research Article is brought to you for free and open access by Journal of Sustainable Mining. It has been accepted for inclusion in Journal of Sustainable Mining by an authorized editor of Journal of Sustainable Mining.

Application of Haines and Terbrugge chart for suitable slope angles – A case study of Artisanal and small-scale mining

Abstract

Significant hazards in Artisanal and small-scale mining (ASM) are rock failure and slope collapse caused by overly steep pit walls, poor mine design and water pressure. There is a lack of expertise and capital in ASM. Providing a simple and cost-effective slope stability analysis and designing systems that can mitigate the risk of slope collapse is essential. This article aims to assess whether stability charts and estimations can be used to establish suitable slope angles to mitigate the overwhelming cases of slope collapse in ASM. The Bieniawski's Rock Mass Rating system and Heins and Terbrugge stability chart were used to assess the stability of Small-scale mine slope and determine suitable slope angles. To validate the reliability of estimations, further analysis was performed through laboratory strength tests to find actual intact rock mass properties and create a model using OPTUM G2 to simulate the Hoek-Brown failure criterion. The study reveals that stability analysis using charts is applicable with the assistance of a rock engineering practitioner after exposing the intact rock mass to map discontinuities. The Heines and Terbrugge chart can be utilized to mitigate slope collapse in ASM, provided that the limitations of the stability graphs are recognized.

Keywords

slope stability, rock collapse, stability charts, numerical modelling, ASM

Creative Commons License



This work is licensed under a [Creative Commons Attribution-Noncommercial-No Derivative Works 4.0 License](https://creativecommons.org/licenses/by-nc-nd/4.0/).

Application of Haines and Terbrugge chart for suitable slope angles – A case study of Artisanal and small-scale mining

Carol Mgiba*, Steven Rupprecht

University of Johannesburg, Department of Mining Engineering and Mine Survey, South Africa

Abstract

Significant hazards in Artisanal and small-scale mining (ASM) are rock failure and slope collapse caused by overly steep pit walls, poor mine design and water pressure. There is a lack of expertise and capital in ASM. Providing a simple and cost-effective slope stability analysis and designing systems that can mitigate the risk of slope collapse is essential. This article aims to assess whether stability charts and estimations can be used to establish suitable slope angles to mitigate the overwhelming cases of slope collapse in ASM. The Bieniawski's Rock Mass Rating system and Heins and Terbrugge stability chart were used to assess the stability of small-scale mine slope and determine suitable slope angles. To validate the reliability of estimations, further analysis was performed through laboratory strength tests to find actual intact rock mass properties and create a model using OPTUM G2 to simulate the Hoek-Brown failure criterion. The study reveals that stability analysis using charts is applicable with the assistance of a rock engineering practitioner after exposing the intact rock mass to map discontinuities. The Heines and Terbrugge chart can be utilized to mitigate slope collapse in ASM, provided that the limitations of the stability graphs are recognized.

Keywords: slope stability, rock collapse, stability charts, numerical modelling, ASM

1. Introduction

The mining industry contributes immensely to the economy and has been the driver of economic development in South Africa [1]. The Minerals Council of South Africa and the Department of Science and Innovation have recently invested in research and innovation projects with the aim of making mining safe and more sustainable. Mining in South Africa comprises of large-scale mining (LSM) and Artisanal and small-scale mining (ASM). Even though ASM is considered ineffective in solving economic problems due to the lack of technical, business and management skills, it still must realize its full potential for a state to achieve Sustainable Development Goals (SDGs) [2]. Recent authors are proposing a shift from viewing ASM as a problematic activity that must be eradicated or phased out to treating it just like LSM through inclusivity and mineral-based sustainable development [1,3]. ASM should be

viewed as an important part of rural livelihood and local development.

The draft policy for ASM in South Africa defines Artisanal and small-scale mining separately. The draft policy [4] defines Artisanal mining as a “traditional and customary mining operation”, making it manual and labor-intensive because of the rudimentary mining methods using rudimentary tools to access the mineral ore, which is usually at shallow depths. Whilst small-scale mining is defined as a prospecting or mining operation that does not employ specialized mining technologies and may not involve large amounts of investment or expenditure. Furthermore, the Minerals and Petroleum Resources Development Act (MPRDA) does not explicitly define ASM but issued a regulation for prospecting and mining permits, in turn defining small-scale mining. A mining permit can be granted for 5 hectares renewable for 3 periods, each not exceeding 1 year. For this study, according to the

Received 20 November 2023; revised 12 May 2024; accepted 5 June 2024.
Available online 8 September 2024

* Corresponding author.
E-mail address: cmgiba@uj.ac.za (C. Mgiba).

<https://doi.org/10.46873/2300-3960.1433>

0022-3468/© Central Mining Institute, Katowice, Poland. This is an open-access article under the CC-BY 4.0 license (<https://creativecommons.org/licenses/by/4.0/>).

MPRDA, the mining operation studied is classified as a small-scale mine.

Artisanal and small-scale mines are owned and operated by the people from the community in an attempt to alleviate poverty and increase the economic value of their livelihood [5,6]. For this reason, individuals living in a village supported by artisanal mining rank it as the most crucial earning activity contributing to household income [7]. ASM occurs in approximately 80 countries worldwide, and about 150 million people depend on ASM (IGF, 2018). The production supply accounts for 80% of global sapphire (used to make jewelry), 20% of gold mining, and 20% of diamond mining from developing countries in Africa, Asia, Oceania, and Central and South America [8]. Due to limited expert knowledge and training, ASM needs assistance in sustaining its immediate environment.

ASM is a hazard to the health and safety of miners and surrounding communities because of the lack of expertise, poor practices in mining, and lack of cost-effective ways to support field excavations [9]. A guide [10] for both small-scale and large-scale mines to meet states that providing technical assistance for small-scale mines is essential. The author adds, “the proposed technologies must be simple, cheap to operate, and easy to maintain.”

The largest share of mining accidents is excavation collapse, and the ground failures can be attributed to a lack of planning, ignoring the nature and types of ground, and the wrong choice of mining methods caused by a lack of mining and rock engineering expertise [9,11,12]. These unsafe conditions cause ASM to be perceived as an unsafe way of mining, which does not consider the health and safety of the mine workers [13]. Conflicts, social unrest, corruption and the likes make ASM difficult to regulate and implement legislation forcing the miners to comply, minimizing the potential harm to miners [14]. Therefore, some unnecessary injuries and fatalities occur that could have been prevented. The health impact is not only limited to the miners and the mines they are working in; communities around these mines are affected by the pollution of water sources surrounding downstream communities and the social impact ASM has on surrounding communities [9,14–16].

The framework that artisanal and small-scale miners operate (i.e., where there is informal working) makes it challenging to propose strategies to mitigate the risk of accidents and protect the health and safety of the miners [17]. Injuries and fatalities caused by ground failure and rock falls are common in ASM. In the report investigating a pit collapse accident [18] noted that the most significant percentage of

accidents occurred, with the highest frequency being pit wall collapse (72%) in 2014. The result from the study shows that the miners affected in the 72 cases ranged between 15 years and upwards, with the oldest being 45 years old. The casualties were 97% male, as most miners were male. It was noted that in the cases where the records existed, the collapse of the mine pit (12.5%) was the most frequent cause of accidents resulting in injuries, followed by explosive blast injuries (9.8%).

It is important to continuously refine critical issues and help establish desirable conditions for ASM operations because it has a high potential to contribute towards sustainable development. Supporting ASM with formalization and other support within the mining cycle can help the Sub-Saharan African government achieve the Sustainable Development Goals (SDGs) targets [19,20]. SDG that can be impacted are:

- SDG 1 No Poverty

ASM began with the initial aim of eradicating poverty within the community. Therefore, it is a platform for wealth creation, job creation, and poverty alleviation.

- SDG 3 Good Health and Well-being

Slope collapse is a significant health and safety hazard. When there are mitigating measures, it directly improves working conditions, which in turn promotes good health and well-being.

- SDG 8 Decent work and economic growth

When slopes collapse, the discovered resource is lost. Slope stability increases the life of the mine, therefore impacting mineral output and revenue realization.

- SDG 9 Industry innovation and infrastructure

Slope stability can assist with introducing mechanization in artisanal mines to upgrade from artisanal to small-scale mining. Mechanization that could be introduced is, for example, blasting – with a stable slope it can be practiced.

Geotechnical engineering is a sub-discipline of civil and mining engineering [21] and focuses on predicting how earth material will behave when disturbed [22]. This prediction is informed by soil mechanics, which dates back to the 1700s. Henri Gautier, a French engineer studied the natural dipping angle of slopes (which we now call the angle of repose). If a slope is stable, the shear

strength is higher than the shear stress; if it is unstable, it is higher than the shear strength. To achieve this balance, Stacey [23] argues that even though there are various components to consider, the one that must be prioritized is how the pit is designed and managed as the mining extraction occurs. This will assist in keeping the excavation stable for as long as the intended life of mine.

There is extensive development of probabilistic empirical-based methods of assessing slope and engineering designs. Quick assessments can be done using the Q-system [24–27] and SMR [28]. Other are Continuous Slope Mass Rating (CoSMR) [29], Rock Mass Rating (RMR) [30] and Slope Stability Rating (SSR) [31]. These are some of the early developments. The methods that have been developed have advantages and limitations, as seen in Table 1. In this study, RMR and SMR are used due to the advantages of stable rock and quick estimations.

Charts can be adopted as a useful tool for preliminary rock slope stability analysis because of their simplicity, though Suorinen et al. [32] consider empirical stability graphs to be highly subjective. Saadoun et al. [33] proclaim that Haines and Terbrugge chart is one of the best-known and most-used charts based on Launscher Modified Rock Mass Rating (MRMR) after Bieniawski Rock Mass Rating (RMR). Depending on the MRMR and slope height, the graph indicates three conclusions: whether the slope angle can be classified using the chart alone, whether the slope stability is marginal when using the chart or whether further analysis is required, as shown in Figure 1.

Applying geomechanics in slopes can clearly assist in limiting the number of slope collapses in ASM. Applying RMR and using the Haines and Terbrugge chart to estimate the slope's safe height and angle at the project's early stages has the potential of being the simple and cost-effective method that can assist in minimizing injuries and fatalities encountered. For this reason, in this study, a small-scale mine was used to demonstrate this process and validate the findings against numerical models. The objective of this paper is to introduce an empirical method used to anticipate failure in slope stability analysis and design in ASM. The implementation of slope stability and design will enable the achievement of Sustainable Development Goals 1, 3, 8 and 9 [19] by mitigating, reducing or eliminating slope collapse in ASM.

2. Material and methods

2.1. Site description

The small-scale mine operation project is located in the eastern lobe of the Bushveld Complex and the Transvaal geological supergroup of South Africa in Steelpoort, Limpopo Province, underlain by sedimentary and volcanic formations, as shown in Figure 2. The silica deposits have thick pegmatite veins adjacent to dykes, which are associated with faulting parallel to the Steelpoort fault, trending southwest to northeast [35]. Within the pegmatite, dense jointing parallel to the indicates shearing after the intrusion.

Table 1. Advantages and limitations of using different types of classification methods in slope stability analysis.

Classifications	Advantages	Disadvantages
(RMR) Rock Mass Rating Kinematic analysis	It determines failure probability and mode of failure. It analyses the quality of the rock mass before excavation design and useful as a guide.	It doesn't include the presence of ground water. It is an empirical method based on competent rock case studies, thus cannot be used for weak rock.
Q-slope	It incorporates all discontinuities, modifies stress reduction factors and accounts for environmental factors that have an influence on the stability of the slope.	It doesn't consider the strength of the rock mass during the analysis. It doesn't consider the effects of the slope height and seismicity on slope stability.
Slope Stability Rating (SSR)	It is effective for slope analysis for those slopes that have closely spaced joints. It considers the effects of seismicity on slope stability.	It doesn't consider the effects of weathering, joint spacing, joint surface condition, or the relationship between joint orientation and slope orientation on the rock mass strength and slope stability.
Slope Mass Rating (SMR)	It considers the effect of failure modes and the relationship between the joint orientation and the slope orientation.	It doesn't consider the impacts of rainfall and the height of the slope when assessing stability. It doesn't consider seismicity impact on slope stability. It is not suitable for slopes with discontinuities close to each other.
Continuous Slope Mass Rating (CoSMR)	It gives an independent, objective rating for each RMR adjustment factor.	It is sensitive to slope characteristics.

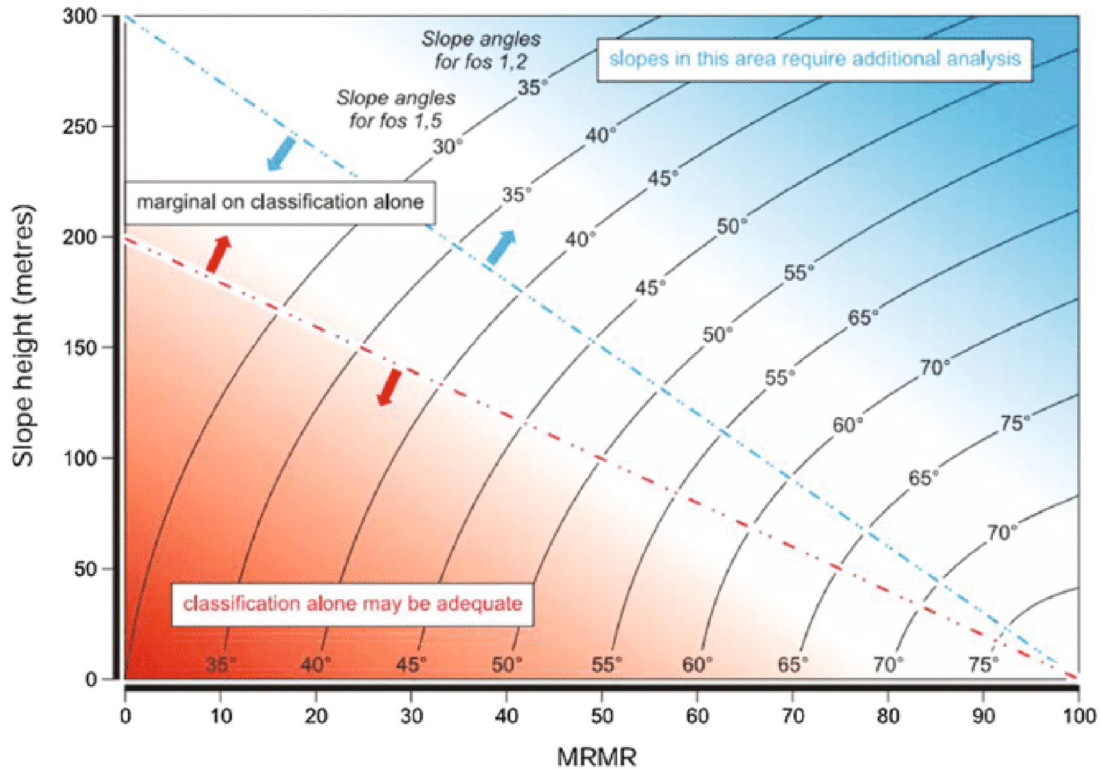


Fig. 1. Design chart used to estimate rock slope stability [34].

The deposit's host rocks comprise of granite, granite sills and gneiss rocks of the Main and Upper Zones of the Bushveld Complex. The project covers the upper part of the Main Zone (MZ) and the Upper Zone (UZ). The Upper Zone comprises the Vanadiferous Titanite-Magnetite, which is disseminated in highly variable, semi-massive, and massive seams of variable thickness. The pegmatite vein system that hosts this deposit continues for several kilometers east and west of the small-scale mining site. Similar veins are known to occur in the hills to the south but have yet to be thoroughly explored and identified.

The mine locality plan of the mining permit project area is shown in Figure 3. The mining permit acquired is for aggregates, silica sand (general) and silica sand (silica) on 5 hectares of portion 10 of the farm Goudmyn 337 KT within the magistrate district of Sekhukhune in Limpopo Province to be mined for two (2) years. The overall mine workings are shown in Figure 4, comprising preliminary open pits on the two deposits: narrower Blue Silica (15–20 m width) and wider White Silica (50–80 m width). The mineral right covers from approximately 850–950 m elevation over a strike length of approximately 480 m. At the time of the study, mining was only conducted using dozer

ripping, free digging with an excavator, and dozing of silica ore slope. However, drilling and blasting were to commence soon, and ramps and roads at practical gradients would be required to permit trucks to transport material from the pit to the crusher at the bottom of the hill.

Dozer ripping has been used in the operation since production commenced. The operation needed to change the excavation approach to drilling and blasting, which can influence the slope's stability. Dozer ripping can effectively loosen the material, but it results in a rough surface with uneven elevations, which can lead to slope instability. Ripping also has the potential to damage the underlying rock mass, which weakens the slope even further.

Drilling and blasting provide greater control over the size and shape of the resulting excavation and allow for a more uniform and predictable slope surface. Blasting can also create fractures and discontinuities in the surrounding rock, leading to instability if the blasts are not carefully designed and executed [23]. Thus, proposing a suitable slope design that can account for blasting is critical, as mining methods play a significant role in the stability of the rock mass.

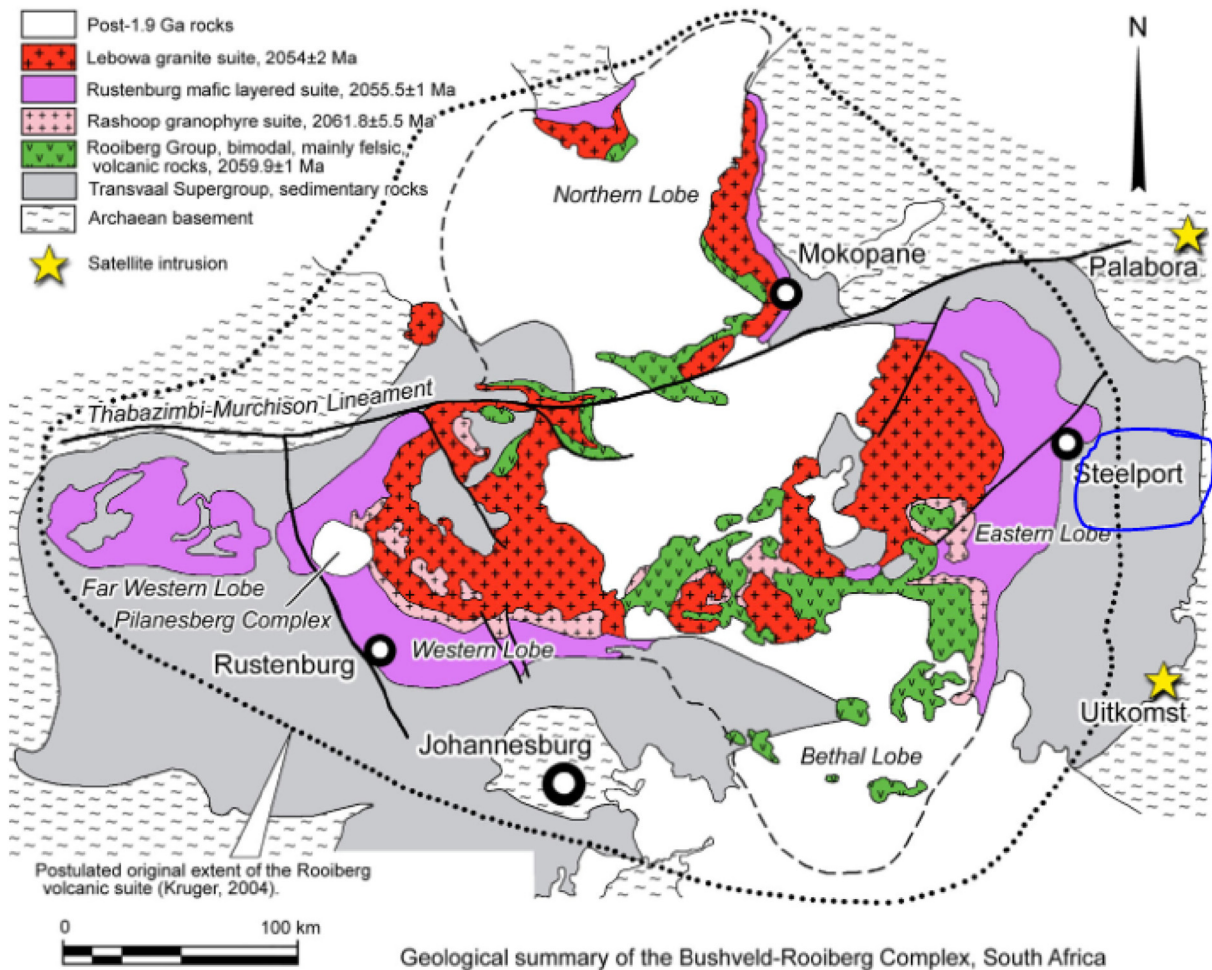


Fig. 2. The bushveld complex [35].

2.2. Geotechnical structural mapping and logging

Mapping for structural analyses was performed on selected areas of the slope, and this involved plotting on the rock mass classification sheet and collecting rock samples. Culshaw [36] suggests that a minimum number of samples per set can be decided site-by-site.

2.3. Laboratory tests

Rock mass samples were collected along the slope through a random probability sampling approach, and then samples were cored to recover core specimens suitable for strength tests at the rock mechanics laboratory. The specimen underwent Uniaxial Compressive Strength (UCS), Triaxial and Brazilian tests. The sampling preparation was conducted in accordance with the International Society of Rock Mechanics (ISRM) suggested methods of laboratory testing:

- The rock samples were inspected and approved for coring. The rocks collected from the slope were sampled by core drilling from the rock, which was the best representation of the rock mass.
- The samples have not had contact with liquids except water. It was, therefore, not contaminated so that the procedure could be carried out.
- Samples were labeled and packed to avoid damage during storage and transportation to the laboratory to preserve integrity.
- It was ensured that proper fittings, o-rings and membranes were used for the tests.
- The core samples were trimmed at the ends and sides carefully.

The following is a description of the specimen according to the requirements of the International Society of Rock Mechanics:

2.3.1. Uniaxial compression strength test

The main purpose of the UCS test is to determine the uniaxial strength of the rock. The specimens

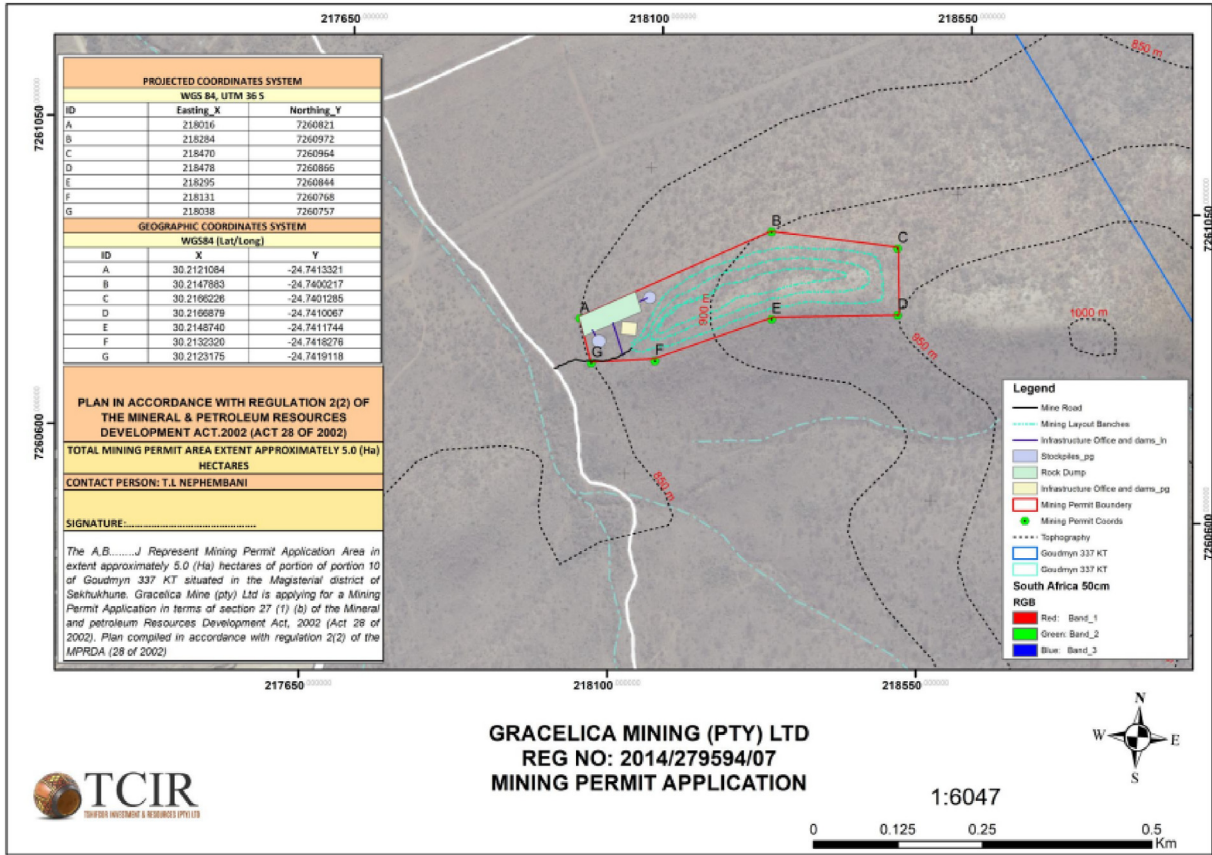


Fig. 3. Locality plan.

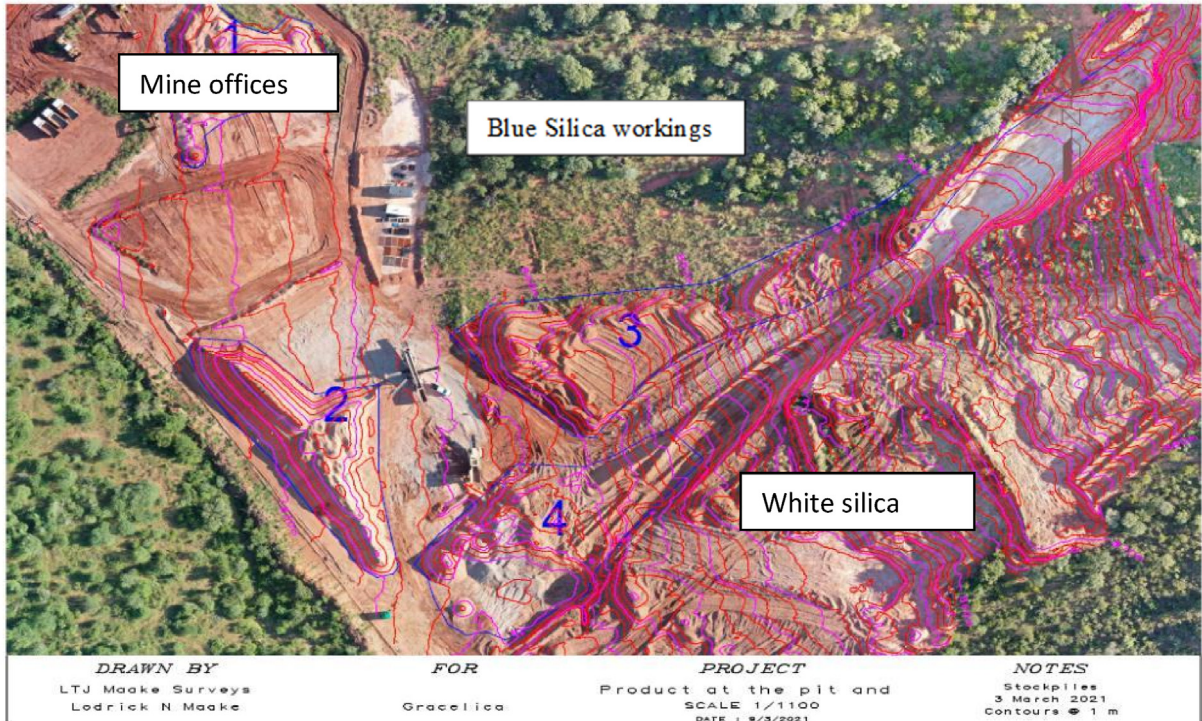


Fig. 4. Plan view of the small-scale mining operation.

were placed in between two stiff compressing platens without lateral confinement. The size of the specimen was a length: diameter ratio of 1 : 0.5 with flat, smooth and parallel to the bar's axis. The specimen deformation measurement was measured and displayed on a computer screen on a stress vs strain curve.

2.3.1.1. Test procedure. A grinding machine prepared the specimen so the ends were parallel and flat. As illustrated in Figure 5(a) and (b), the specimen's side must be smooth and devoid of imperfections from top to bottom. Every surface of the specimen had to be smooth.

The specimen attached with gauges; the axial constant load is applied by servo-hydraulic load machine until the specimen fails. UCS is then determined by load divided by cross-sectional area of the specimen.

2.3.1.2. Data captured. When the rock specimen was loaded and connected to the machine and the computer, the machine is closed, the computer is prepared for readings, and the start button is pressed. While the test is in session, the stress versus strain graph is generated together with the modulus vs. stress curves and poisons ratio vs. stress curves, as seen in Figures 6(a), (b) and (c).

2.3.2. For the triaxial shear strength test

The main purpose of the triaxial shear strength test is to determine the Mohr-Coulomb cohesion friction strength and friction angle as close as possible to rockmass confinement conditions, the unconfined compressive strength from the

deduction of confined failure strengths and Young's modulus and Poisson's ration. This was done through a Single Stage Triaxial tests, where each specimen was tested at different confinements. The samples' length: height ratio was 1 : 0.5.

2.3.2.1. Test procedure. In the triaxial test each specimen is confined in a cell where pressure is applied to the surrounding sleeve together with the axial stress along the axis of the specimen. The confining stress surrounding the sleeve is kept constant and increases with each sample. At each confining stress, axial stress is increased by constant loading until failure occurs. Post-yield stress-strain behavior is defined through the axial strain vs axial stress curve generated as the load is applied. The confining pressure was incremented by 5 MPa for each specimen.

2.3.2.2. Data captured. The Mohr-Coulomb circles represent a state of shear stress and normal stress at a point, and the circumference of each circle represents the shear and normal stress on different planes during the test. The red line represents the Mohr failure obtained at different stresses (see Fig. 7).

2.3.3. Indirect tensile strength test (Brazilian test)

The indirect tensile strength was determined using the Brazilian disk test shown in Figure 8. This test was carried out using a core disk cut with a thickness of half of the diameter.

2.3.3.1. Test procedure. The core disk was cut from a vertical plug sample with a diameter: height ratio of

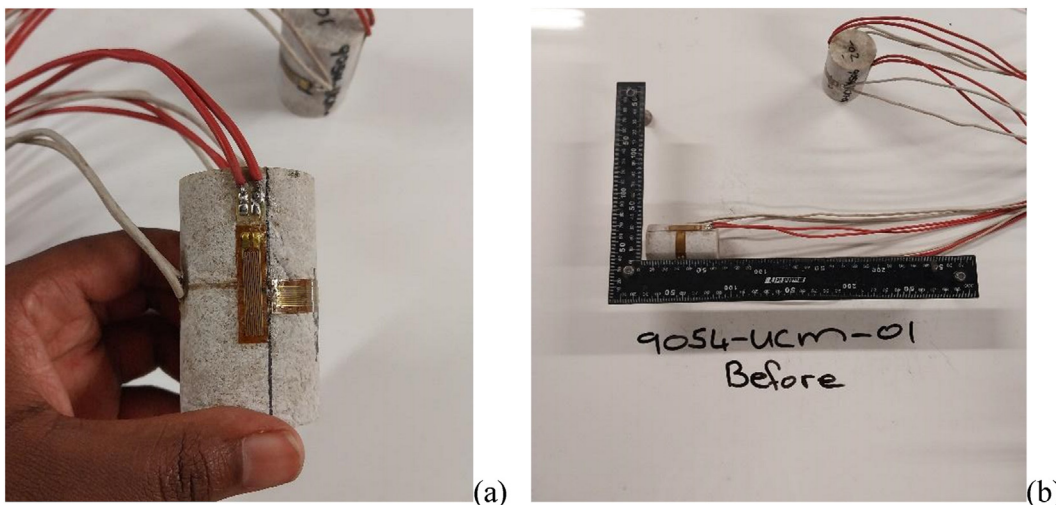


Fig. 5. (a) Specimen connected to terminal measuring vertical displacement, (b) specimen connected to terminal measuring horizontal displacement.

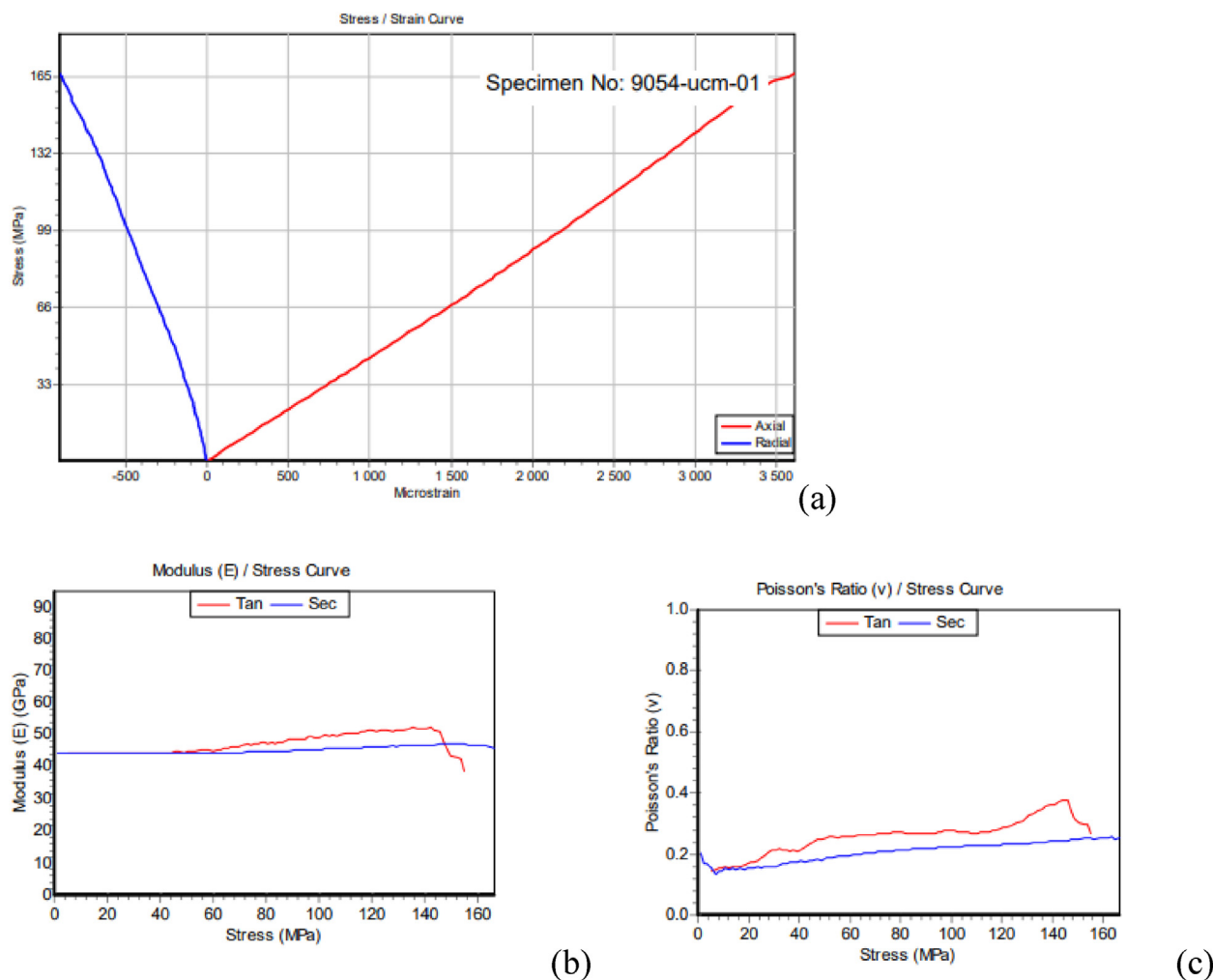


Fig. 6. (a) Uniaxial compression strength test, (b) with modulus elasticity, (c) with poisons ratio.

1 : 0.5. The disk is then located between parallel steel platens with strips that spread the load along each edge and over the circumference of the disk. When the specimen fractures or splits at the center, it is recorded using a microprocessor system.

3. Results and discussion

3.1. Geotechnical structural mapping and logging results

Geotechnical structural mapping results sample areas are shown in Figures 9–12. The slope showed considerable jointing, with the primary joint set (Set 1) running parallel to the pegmatite and resulting in slabbing of the highwall, as shown in Figure 4. Various cross-joint sets (Sets 2 to 4) are present, assisting in the loose slab hazard posed by this wall, which is 12 m high at the time of mapping. Cross-jointing sets present wedge failure and play a significant role in slope stability assessment [37].

The dyke was exposed at the top of the Blue Silica pit, where it cuts north across the pegmatite. It is highly weathered and of lower material strength than the pegmatite assumed to have a similar system of joints to those observed in Figures 5 and 6; the exposure was too small and too weathered to be completely sure of its visibility at the highwall (see Figs. 9 and 10). Weathering is a geological process that shows that there are instabilities' movements occurring within the rock mass due to the process of weathering and cementation [38].

No highwalls were developed within the White Silica pit, and the contacts with the dyke that separates the Blue and White Silica sections are poorly exposed along a trench at the 890 m elevations, as illustrated in Figure 11. The dyke appears highly weathered with deeper brown soil cover, and there is a sharp step into the stronger quartz pegmatite.

The rock mass geotechnical characteristics were defined to assess pit slope angles and potential

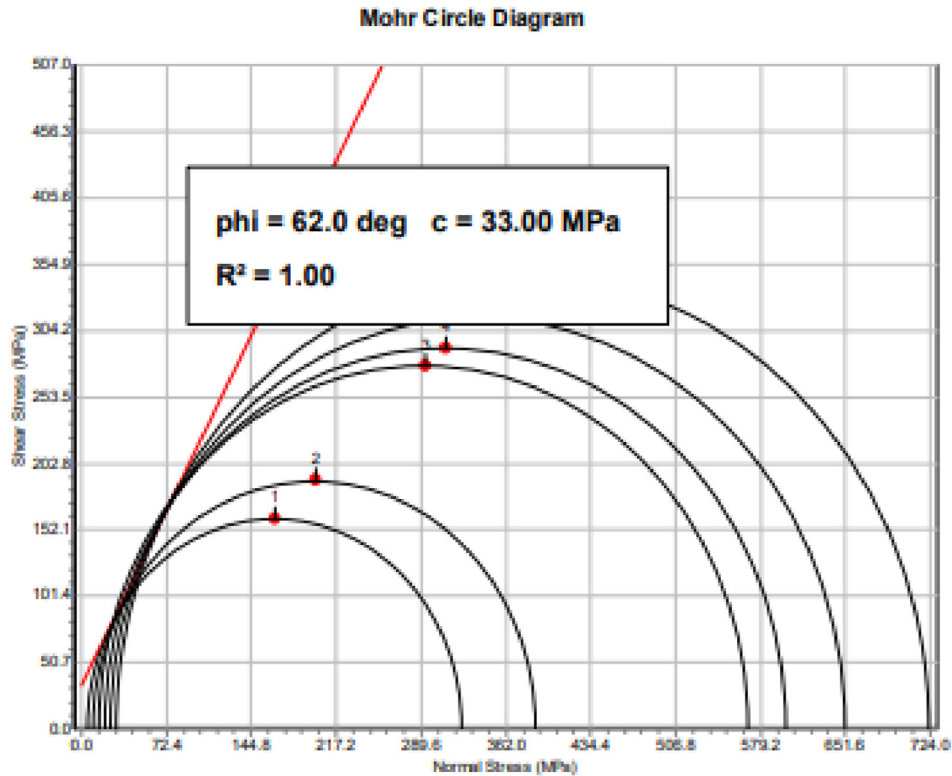


Fig. 7. Triaxial compressive strength test data captured.



Fig. 8. Specimen prepared for indirect tensile strength (Brazilian test).

hazards. A preliminary estimate using system of an overall rock mass rating (RMR) [39] was used, then an estimate of the overall stable slope angle for the walls of the pit using the chart shown in Figure 1.

The adjusted Rock Mass Rating is 42; therefore, the rock mass class is No. III, meaning that the slope is developed in fair rock. The RMR and Adjusted RMR were plotted on the design chart developed by Haines and Terbrugge's design chart based on case studies on stable and failed slopes. The expected pit depths will be approximately 20 m below the pre-

mining ground surface, giving a highwall height of approximately 20 m.

Using Figure 1, a slope height of 20 m and adjusted MRMR of 42, slope angles in the 52–57° range are considered potentially stable using classification alone. The data plot within a region of the chart where it is safe to expect overall stability based on an MRMR plotted on the chart assessment alone. The current slope angle is, however, about 75–80° expected to reach 20 m height; therefore, this angle versus height plots within a region where further

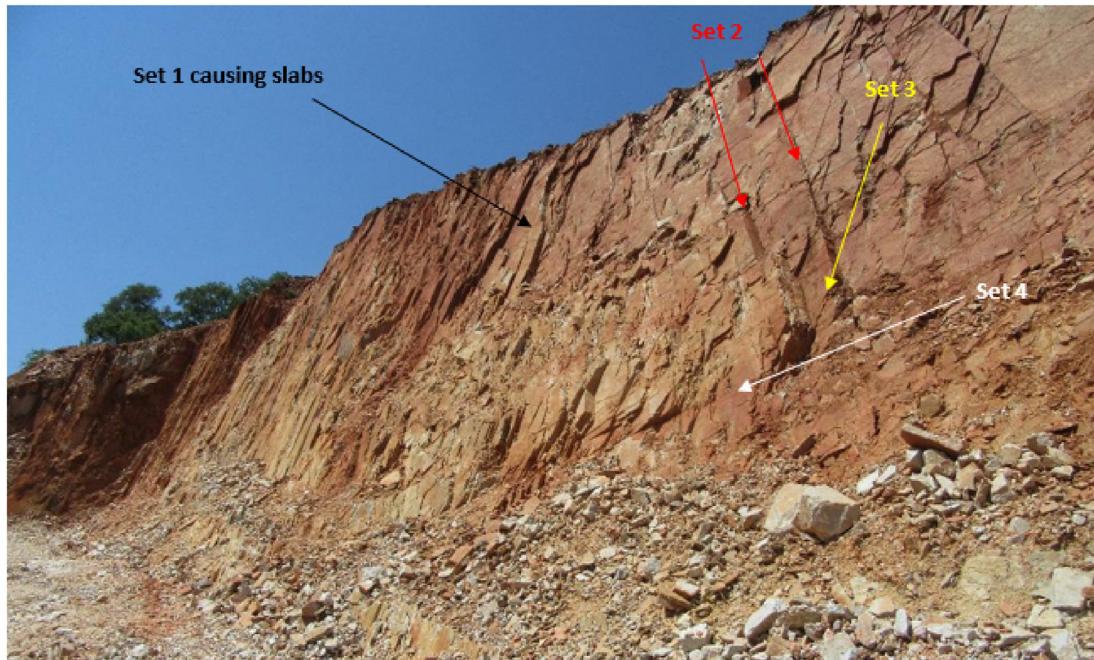


Fig. 9. Highwall mapping (Sample 1).

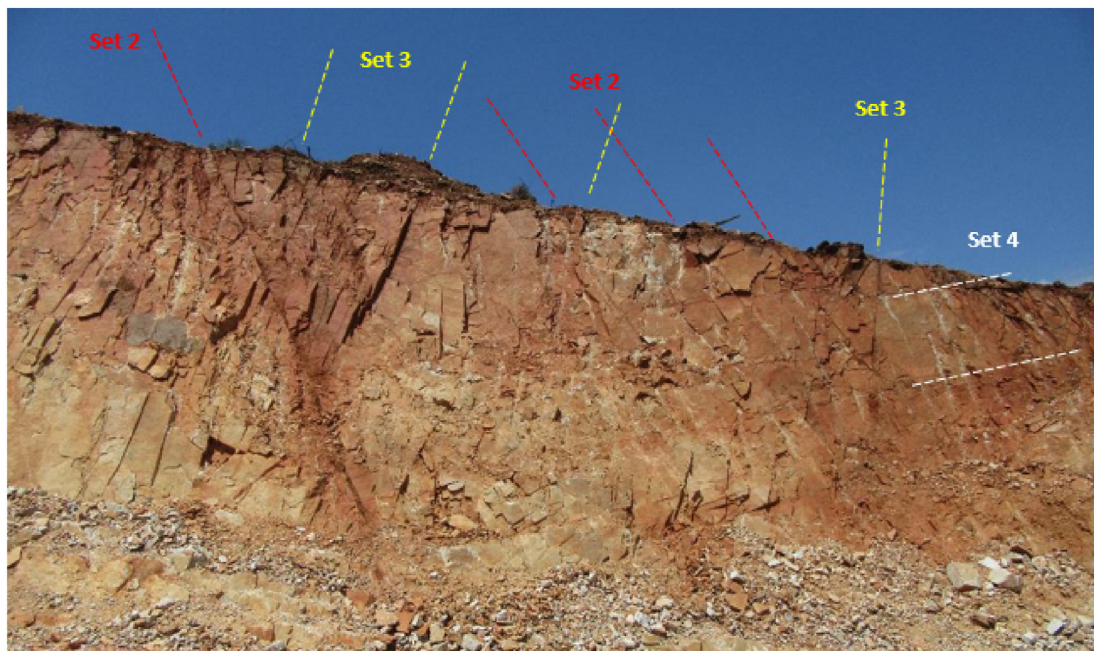


Fig. 10. Highwall mapping (Sample 2).

alternative detailed analysis is considered necessary. Further laboratory analysis and model construction was completed to simulate possible failure and propose a new mining method. The parameters of original shear strength are reduced using strength reduction techniques until the slope failure occurs.

RMR was then compared to SMR, which has been widely used as a rapid method to assess slope stability. Joint set 4 represents an opportunity for planar failure as it is dipping at approximately 30° (see Fig. 6); F1 is thus 0.40. Joint sets 2 and 3 show a possibility of wedge failure occurring; F2 is 1.00 as the angles of the joints are more than 45° . F3 is

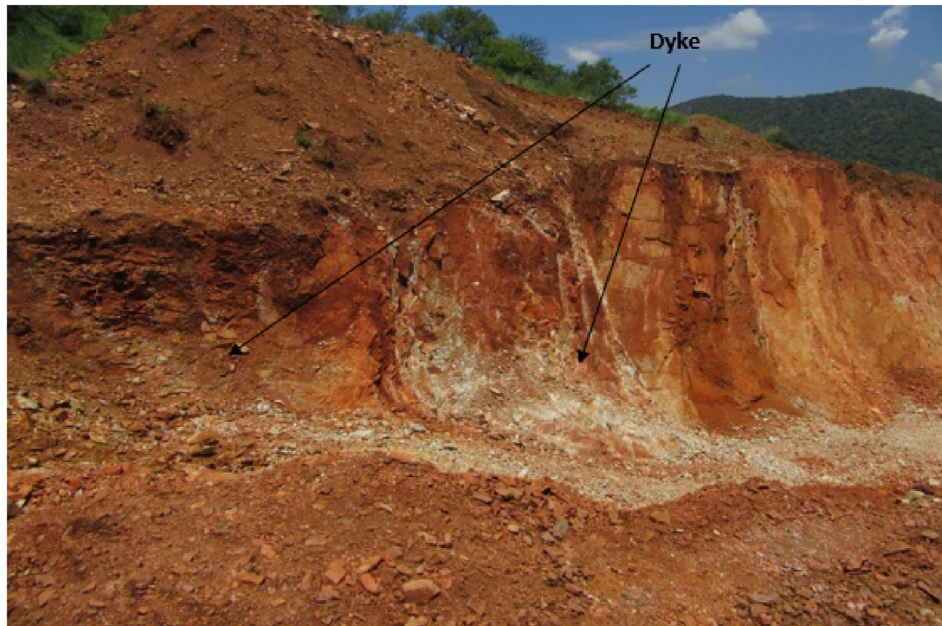


Fig. 11. Highwall mapping (Sample 3).

0 because the angle of joint set 4 (which are parallel to each other) is greater than 10° . Since the project will be extracting the ore using the blasting mining method, F_4 is 0.

$$\text{SMR} = \text{RMR} + (F_1 \times F_2 \times F_3) + F_4$$

$$\text{SMR} = 42 + (0.40 \times 1 \times 0) + 0 = 42$$

SMR class III, which means the slope is normal with partial stability with wedge; failure probability of 0.4.

3.2. Laboratory results

The results of the uniaxial compressive strength (UCS) of the specimen ranged between 142 and 166 MPa, failure load between 202 and 241 kN,



Fig. 12. Highwall mapping (Sample 4).

tangent elastic modulus at 50% UCS is between 47 and 48 GPa, secant elastic modulus at 50% UCS is between 45 and 47 GPa, Poisson’s ratio tangent at 50% UCS is between 0.27 and 0.29, Poisson’s ratio secant at 50% UCS is between 0.22 and 0.27 as shown in [Table 2](#).

The results of the triaxial compressive strength at 5 MPa increments of confining pressure from 5 to 30 MPa is between 325 and 724 MPa, cohesion is 33 MPa and friction angle 62°, as shown in [Table 3](#). Failure code XA, which is not influenced by discontinuities, denotes that a single sliding failure occurred during specimen failure, which occurred in all specimens tested.

The Brazilian tensile strength test results range between 9.1 and 9.7 MPa for the specimens tested, as shown in [Table 4](#). B denotes that failure occurred

within intact rock, not on existing joints or discontinuities ([Table 4](#)).

3.3. Numerical modelling

Optum G2 is an ideal software tool to use for shallow foundation analysis and design because it provides a means for determining bearing capacities efficiently. It allows computing the upper and lower limits to find a suitable solution in between the limits. Therefore, verification is built-in, providing numerical verification. The Optum G2 numerical verification through models was used to supplement empirical methods.

Optum G2 numerical modelling software was used to run the mesh, initial stresses, and strength reduction analysis to see the stress and the strain

Table 2. Results of UCS with elastic modulus and poisson ratio measured using strain gauges.

Specimen no. 9054-	Specimen dimensions					Specimen test results						
	Diameter (D) mm	Height (H) mm	Ratio (H : D)	Mass g	Density g/cm ³	Failure load kN	Strength (UCS) MPa	Tangent elastic modulus at 50% UCS GPa	Secant elastic modulus at 50% UCS GPa	Poisson’s ratio tangent at 50% UCS	Poisson’s ratio secant at 50% UCS	Linear axial strain at failure mm/mm
UCM-01	43.01	60.17	1.40	227.16	2.60	241.8	166.4	47.4	45.0	0.27	0.22	0.003611
UCM-02	42.47	63.97	1.51	234.75	2.59	202.5	142.9	48.3	46.8	0.29	0.27	0.003065

Table 3. Results of triaxial compressive strength tests.

Specimen No. 9054-	Specimen dimensions					Specimen test results					
	Diameter (D) mm	Height (H) mm	Ratio (H : D)	Mass g	Density g/cm ³	Confining pressure δ3 MPa	Failure load P kN	Strength (TCS) δ1 MPa	Mohr Coulomb		Failure code
									Cohesion MPa	Friction angle deg.	
TCS-01	42.91	69.3	1.6	260.7	2.60	5.0	470.4	325.3	33.0	62.0	XA
TCS-02	43.06	72.4	1.7	274.4	2.60	10.0	566.6	389.1			XA
TCS-03	42.24	50.9	1.2	186.0	2.61	15.0	798.9	570.1			XA
TCS-04	43.39	78.2	1.8	301.8	2.61	20.0	890.6	602.3			XA
TCS-05	42.12	79.5	1.9	287.1	2.59	25.0	909.3	652.6			XA
TCS-06	42.17	72.9	1.7	264.9	2.60	30.0	1011.1	723.9			XA

Table 4. Results of Brazilian tensile strength tests.

Specimen No. 9054-	Specimen dimensions				Specimen test results		
	Diameter mm	Height mm	Mass gram	Density g/cm ³	Failure load	Brazilian tensile strength MPa	Note
UTB-01	43.10	22.60	84.52	2.56	13.9	9.1	B
UTB-02	43.42	21.58	82.68	2.59	14.3	9.7	B

Table 5. Properties of the intact rock.

Lithology	RQD	GSI	Density (t/m ³)	σ _t (MPa)	σ _c (MPa)	E _m (GPa)	φ°	C (MPa)
Quartzite	110	55	2.6	723	166	47	62	33

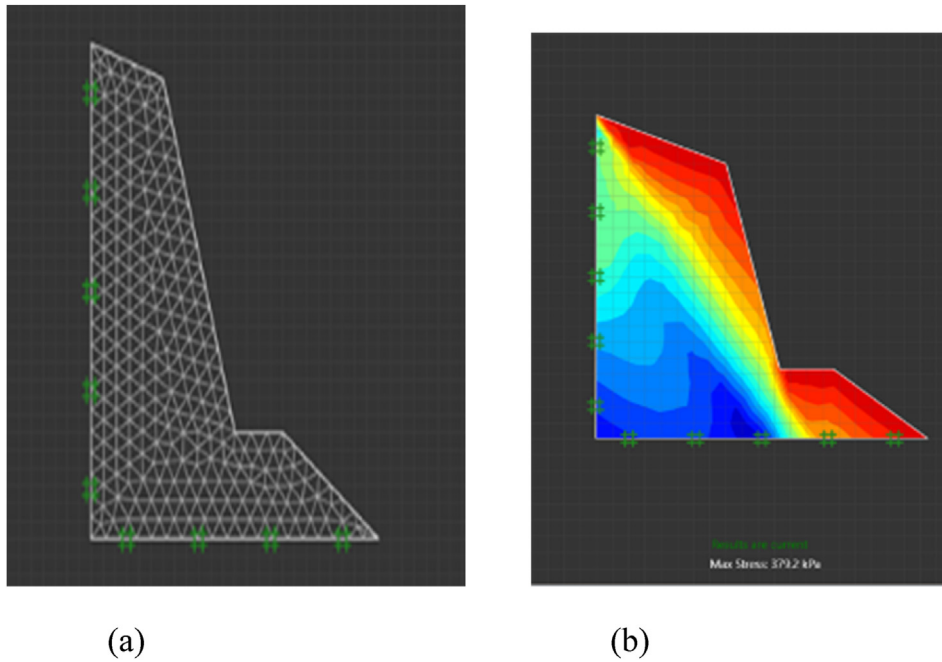


Fig. 13. (a) Stage 1: Mesh simulation, (b) Stage 3: Initial stresses acting on slope.

that the slope will experience once the excavation depth has reached 20 m. Table 5 summarizes mechanical properties that were input into OPTUM G2.

As seen in Figure 13(a), the slope model is created with support as the slope is on the hillside, which serves as an anchor of support. The mesh size was

set to 1000 elements to increase accuracy. Before running the analysis, the initial stress was determined because it is an important aspect of strength and deformation analysis. Initial stress σ_1 that the slope experiences can be seen in Figure 13(b). If the mine continues to mine to 20 m depth, high stress

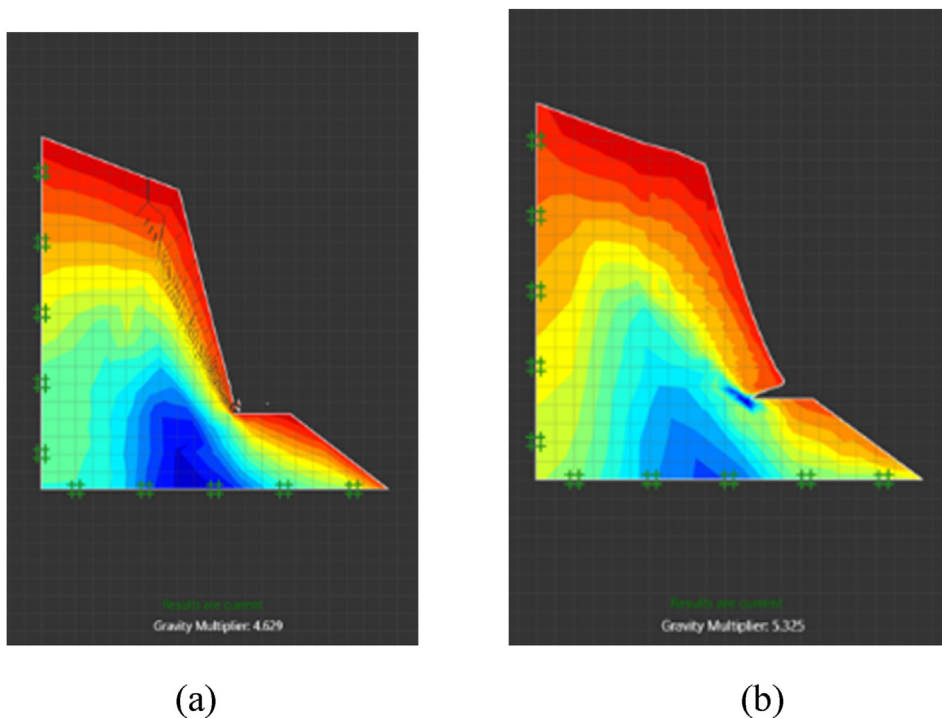


Fig. 14. Illustration of slope deformation: (a) lower limit of gravity impact on the slope, (b) upper limit of gravity impact on the slope.

will be experienced at the top of the slope and the working bench floor.

Stage 5 of the model ran a Limit analysis, as seen in Figure 14(a), to assess the stability capacity of geological structures in the slope. Fixed and

Multiplier loads were applied where the fixed load was kept constant, and the multiplier load was amplified until collapse. From Figure 14, the slope deformation occurred where the gravity multiplier was 4.63 for the lower limit and 5.33 for the upper limit before possible collapse occurred.

Figure 15 shows the strength reduction factor generated at stage 7. The strength reduction analysis determines the strength that is needed to prevent collapse given a set of actual loads. For Hoek-Brown Criterion, UCS and intact rock parameter factors are reduced. The strength reduction factor for this slope is 2.97.

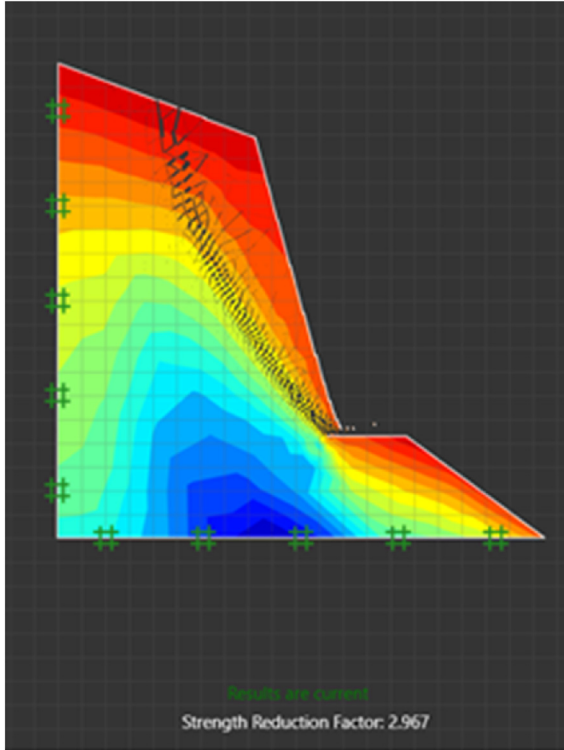


Fig. 15. Model after strength reduction analysis with a reduction factor of 2.9.

3.4. Proposed mining method

According to the findings, the highwall slope angle was too steep for the MRMR classification. Further analysis was done for the actual slope angle through a numerical model, and the highwall of +70° of a pegmatite quartzite material showed high stresses at the slope’s peak.

Therefore, a recommendation is that in order to adopt a pit slope angle of 52 to 57° at a pit depth of 20 m, mining must follow a 5 m benching system with the following parameters:

- a) Bench width 2.5 m.
- b) Bench face angle: 75–80°.
- c) Drilling steps off from highwall: 3.5 m.

The bench face angle is anticipated to be achieved through minor back breaks on joints in the rock

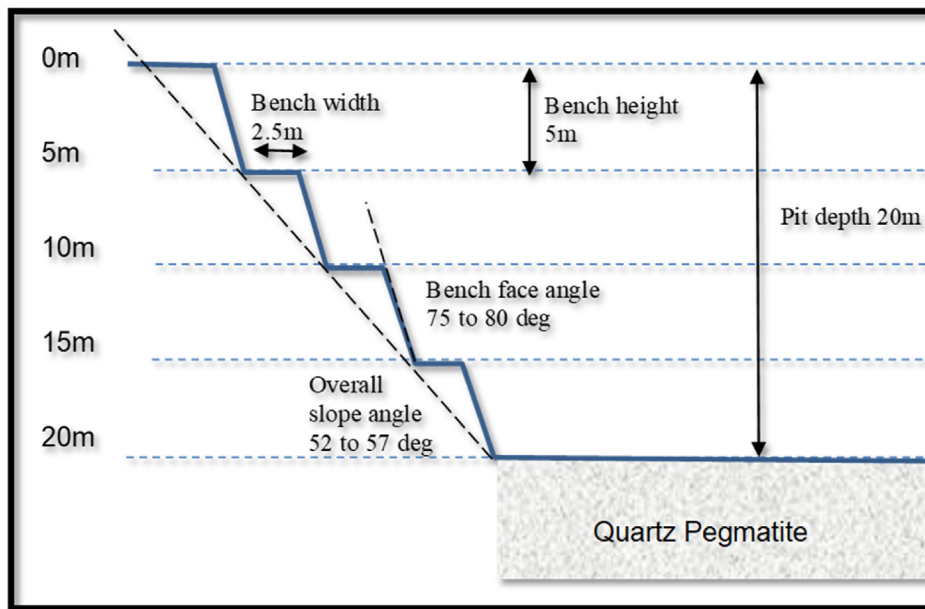
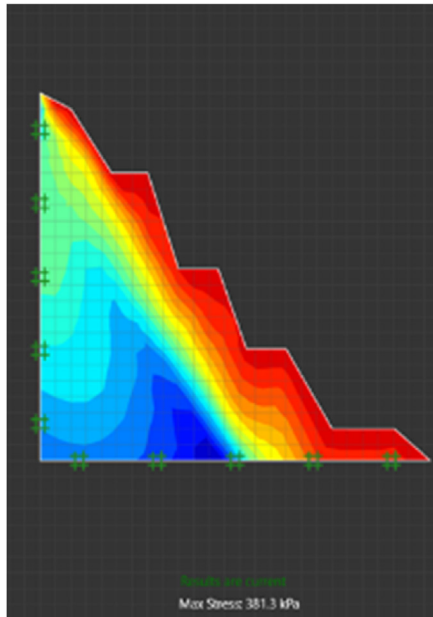


Fig. 16. Proposed bench mining geometry.

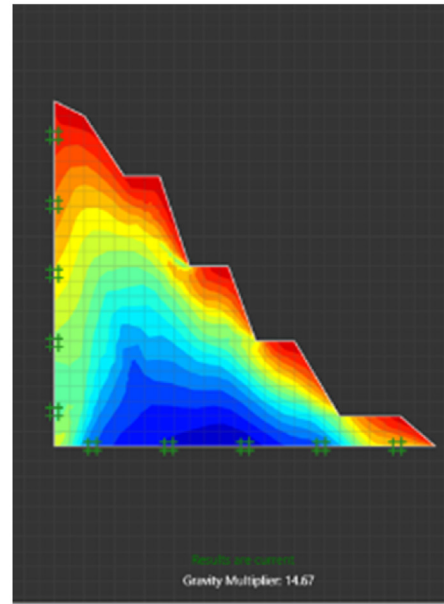
mass and would not require angled pit perimeter holes. This proposed geometry is illustrated in Figure 16, and the displacement stability analysis is given in Figure 16.

The proposed bench mining geometry model showed that the maximum stress has slightly

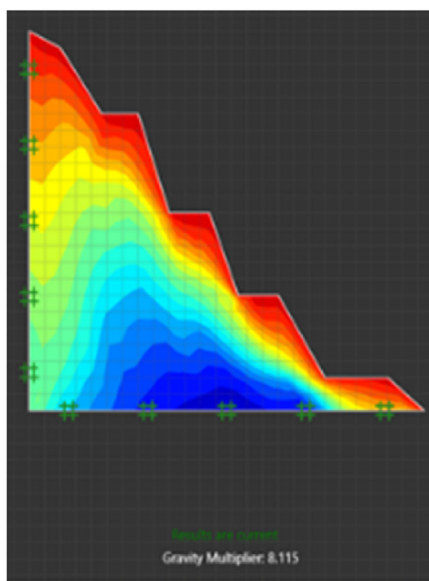
increased to 381 kPa as seen in Figure 17. Figure 17(a) and (b) shows that the gravity multiplier has increased to 14.67 for the upper limit and 8.12 for the lower limit of the limit equilibrium analysis. Figure 17(c) and (d) shows that the strength reduction factor rises to 4.47.



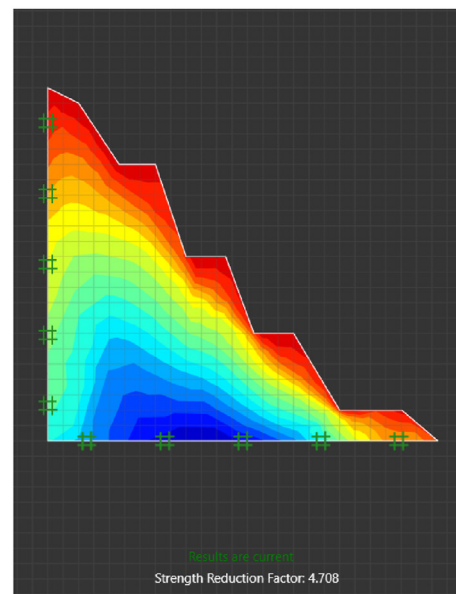
(a)



(b)



(c)



(d)

Fig. 17. Bench mining design stability analysis: (a) Maximum stress, (b) Gravity multiplier upper limit, (c) Gravity multiplier lower limit, (d) Strength reduction factor.

4. Conclusion

There have been various methods introduced in slope stability to make the process of evaluating the stability of a slope rapid and reliable. These methods can assist in providing a rapid assessment of a slope. This paper demonstrated the process of assessing slope stability, and the SMR and RMR were validated using laboratory testing and numerical modelling. In the case studied the initial slope angle and height derived from the Heines and Tebrugge design graph revealed that the slope angle is too steep for the initial mining method. The numerical model of the proposed bench mining showed that the gravity multiplier has increased to 14.67 for the upper limit and 8.12 for the lower limit of the limit equilibrium analysis.

The key findings are:

- The Haines and Terbrugge's chart can be a valuable tool for ASM in mitigating slope collapse.
- Bench mining is a safe mining method that small-scale surface miners can use to minimize slope collapse.
- The empirical method is a cost-effective method that can be used in ASM with guidance from an experienced Rock engineer.
- Sustainability can be further established by training artisanal and small-scale miners in assessing slope stability.

Ethical statement

The authors state that the research was conducted according to ethical standards.

Funding body

This research received no external funding.

Conflicts of interest

The authors declare no conflict of interest.

Acknowledgements

The authors would like to thank Associate Professor Onifade Moshood for guidance, writing assistance and proofreading the manuscript.

References

- [1] Mutemeri N, Walker JZ, Coulson N, Watson I. Capacity building for self-regulation of the Artisanal and Small-Scale Mining (ASM) sector: a policy paradigm shift aligned with development outcomes and a pro-poor approach. *Extr Ind Soc* 2016;3(3). <https://doi.org/10.1016/j.exis.2016.05.002>.
- [2] Laing T, Moonsammy S. Evaluating the impact of small-scale mining on the achievement of the sustainable development goals in Guyana. *Environ Sci Pol* 2021;116. <https://doi.org/10.1016/j.envsci.2020.11.010>.
- [3] Ledwaba PF. The status of artisanal and small-scale mining sector in South Africa: tracking progress. *J S Afr Inst Min Metall* 2017;117(1):33–40. <https://doi.org/10.17159/2411-9717/2017/v117n1a6>.
- [4] Mantashe SG. General notices • alGemene KennisGewinGs department of mineral resources and energy notice 258 of 2021. 2021. www.gpwonline.co.za.
- [5] Debrah AA, Watson I, Quansah DPO. Comparison between artisanal and small-scale mining in Ghana and South Africa the regional frameworks: Yaoundé Vision and the MMSD in the AMV. *J S Afr Inst Min Metall* 2014;114.
- [6] Hentschel T, Hruschka F, Priester M. Global report on artisanal and small-scale mining. In: *Mining, minerals and sustainable development*; 2002.
- [7] Kamlongera PJ. Making the poor “poorer” or alleviating poverty? Artisanal mining livelihoods in rural Malawi. *J Int Dev* 2011;23(8). <https://doi.org/10.1002/jid.1836>.
- [8] Rodríguez-Novoa F, Holley E. Coexistence between large-scale mining (LSM) and artisanal and small-scale mining (ASM) in Perú and Colombia. *Resour Pol* 2023;80. <https://doi.org/10.1016/j.resourpol.2022.103162>.
- [9] Bansah KJ, Yalley AB, Dumakor-Dupey N. The hazardous nature of small scale underground mining in Ghana. *J Sust Min* 2016;15(1):8–25. <https://doi.org/10.1016/j.jsm.2016.04.004>. Central Mining Institute in Katowice.
- [10] The World Bank. *Minin together: large- scale mining meets Small-scale mining- A guide for action*. 2009.
- [11] Moloi M, Zvarivadza T. Investigating slope failure and rockfall controls at a South African coal mine. In: *6th intl conference on computer applications in the minerals industries*, October; 2016.
- [12] Mametja TD, Zvarivadza T. Slope stability enhancement through slope monitoring data interpretation. In: *51st US rock mechanics/geomechanics symposium 2017*. vol. 5; 2017.
- [13] Lu JL. Occupational health and safety in small scale mining: focus on women workers in the Philippines. *J Int Wom Stud* 2012;13(3).
- [14] Zvarivadza T. Artisanal and small-scale mining as a challenge and possible contributor to sustainable development. *Resour Pol* 2018;56. <https://doi.org/10.1016/j.resourpol.2018.01.009>.
- [15] Mimba ME, Mbafor PUT, Nguemhe Fils SC, Nforba MT. Environmental impact of artisanal and small-scale gold mining in East Cameroon, Sub-Saharan Africa: an overview. *Ore Energy Resource Geol* 2023;15. <https://doi.org/10.1016/j.oreoa.2023.100031>.
- [16] Zvarivadza T. Large scale miners - communities partnerships: a plausible option for communities survival beyond mine closure. *Resour Pol* 2018;56. <https://doi.org/10.1016/j.resourpol.2017.12.005>.
- [17] Elenge MM, De Brouwer C. Identification of hazards in the workplaces of artisanal mining in Katanga. *Int J Occup Med Environ Health* 2011;24(1):57–66. <https://doi.org/10.2478/s13382-011-0012-4>.
- [18] Walrond G, Bayah J, Sparman C, Hall G. 040815_COI Report_Final. 2015.
- [19] Hilson G, Hilson A, Maconachie R. Opportunity or necessity? Conceptualizing entrepreneurship at African small-scale mines. *Technol Forecast Soc Change* 2018;131. <https://doi.org/10.1016/j.techfore.2017.12.008>.
- [20] Hilson G, Maconachie R. Artisanal and small-scale mining and the sustainable development goals: opportunities and new directions for sub-Saharan Africa. *Geoforum* 2020;111. <https://doi.org/10.1016/j.geoforum.2019.09.006>.
- [21] Robbins BA, Stephens JJ, Marcuson WF. *Geotechnical engineering*. *Encycl Geol* 2020;1-6. <https://doi.org/10.1016/B978-0-12-409548-9.12508-4>. Second Edition (Vol. 6).
- [22] Das B, Sawicki A. Fundamentals of geotechnical engineering. *Appl Mech Rev* 2001;54(6). <https://doi.org/10.1115/1.1421116>.

- [23] Stacey T. Safety in mines research advisory committee final report best practice rock engineering handbook for “other” mines. 2001.
- [24] Barton N, Lien R, Lunde J. Using the Q-system: rock mass classification and support design. Norwegian Geotechnical Institute; 1974.
- [25] Kouhdaragh M, Azarafza M, Derakhshani R. A Qslope-based empirical method to stability assessment of mountain rock slopes in multiple faults zone: a case for North of Tabriz. *MethodsX* 2022;9. <https://doi.org/10.1016/j.mex.2022.101718>.
- [26] Mao Y, Chen L, Nanekaran YA, Azarafza M, Derakhshani R. Fuzzy-based intelligent model for rapid rock slope stability analysis using qslope. *Water (Switzerland)* 2023;15(16). <https://doi.org/10.3390/w15162949>.
- [27] Tao H, Xu G, Meng J, Ma R, Dong J. Stability assessment of high and steep cutting rock slopes with the SSPC method. *Adv Civ Eng* 2021;2021. <https://doi.org/10.1155/2021/8889526>.
- [28] Romana M. The geomechanical classification SMR for slope correction. In: 8th ISRM congress; 1995.
- [29] Tomás R, Delgado J, Serón JB. Modification of slope mass rating (SMR) by continuous functions. *Int J Rock Mech Min Sci* 2007;44(7). <https://doi.org/10.1016/j.ijrmms.2007.02.004>.
- [30] Bieniawski ZT. The rock mass rating (RMR) system (geomechanics classification) in engineering practice. ASTM Special Technical Publication; 1988. STP 984. <https://doi.org/10.1520/STP48461S>.
- [31] Taheri A, Tani K. Rock slope design using Slope Stability Rating (SSR) - application and field verifications. In: Proceedings of the 1st Canada-US rock mechanics symposium - rock mechanics meeting society’s challenges and demands. vol. 1; 2007. <https://doi.org/10.1201/noe0415444019-c27>.
- [32] Suorineni FT, Kaiser PK, Tannant DD. Likelihood statistic for interpretation of the stability graph for open stope design. *Int J Rock Mech Min Sci* 2001;38(5). [https://doi.org/10.1016/S1365-1609\(01\)00033-8](https://doi.org/10.1016/S1365-1609(01)00033-8).
- [33] Saadoun A, Hafsaoui A, Fredj M. Landslide study of lands in quarries. Case choug amar - M’sila, Algeria. In: Sustainable Civil Infrastructures; 2018. https://doi.org/10.1007/978-3-319-61612-4_3.
- [34] Haines A, Terbrugge PJ. Preliminary estimation of rock slope stability using rock mass classification systems. In: 7th ISRM Congress; 1991. [https://doi.org/10.1016/0148-9062\(93\)92931-f](https://doi.org/10.1016/0148-9062(93)92931-f).
- [35] Molyneux TG. A geological investigation of the bushveld complex in sekhukhune land and part of the Steelpoort valley. In: Transactions of the geological society of South Africa. vol. 77; 1974.
- [36] Culshaw MG. Ulusay, R (ed.), 2015. The ISRM suggested methods for rock characterization, testing and monitoring: 2007–2014. *Bull Eng Geol Environ* 2015;74(4). <https://doi.org/10.1007/s10064-015-0780-3>.
- [37] Chen L, Zhang W, Zheng Y, Gu D, Wang L. Stability analysis and design charts for over-dip rock slope against bi-planar sliding. *Eng Geol* 2020;275. <https://doi.org/10.1016/j.enggeo.2020.105732>.
- [38] Azarafza M, Hajjalilue Bonab M, Derakhshani R. A novel empirical classification method for weak rock slope stability analysis. *Sci Rep* 2022;12(1). <https://doi.org/10.1038/s41598-022-19246-w>.
- [39] Bieniawski ZT. Rock mass classifications in rock engineering. vol. 1; 1977. [https://doi.org/10.1016/0148-9062\(77\)90608-8](https://doi.org/10.1016/0148-9062(77)90608-8).